

# A spatially explicit reconstruction of cropland cover in China from 1661 to 1996

Shicheng Li · Fanneng He · Xuezheng Zhang

Received: 19 May 2014 / Accepted: 18 December 2014 / Published online: 14 January 2015  
© Springer-Verlag Berlin Heidelberg 2015

**Abstract** Reconstruction of cropland cover is crucial for assessing human impact on the environment. In this study, based on existing studies concerning historical cropland, population data and government inventories, we obtained a provincial cropland area dataset of China for 1661–1996 via collection, revision and reconstruction. Then, the provincial cropland area was allocated into grid cells of  $10 \times 10$  km depending on the land suitability for cultivation. Our reconstruction indicates that cropland increased from  $\sim 55.5 \times 10^4$  km<sup>2</sup> in 1661 to  $\sim 130.0 \times 10^4$  km<sup>2</sup> in 1996. From 1661 to 1873, cropland expanded tremendously in the Sichuan Basin, and land reclamation was greatly enhanced in North China Plain. For 1873–1980, agricultural development occurred primarily in northeastern China. After 1980, most provinces in the traditionally

cultivated region of China experienced decreases in cropland area. In comparison with satellite-based data for 2000, we found that our reconstruction generally captures the spatial distribution of cropland. Also, differences are mostly  $<20\%$  ( $-20$  to  $20\%$ ). Compared with HYDE 3.1 dataset, which is designed for the global scale, our model is more suitable for reconstructing the historical crop cover of China at  $10 \times 10$  km grid scale. Our reconstruction can be used in climate models to study the impact of crop cover change on the climate and carbon cycle.

**Keywords** Historical cropland cover · Spatially explicit · Reconstruction · Land suitability for cultivation

---

Editor: Will Steffen.

---

S. Li · F. He (✉) · X. Zhang  
Key Laboratory of Land Surface Pattern and Simulation,  
Institute of Geographic Sciences and Natural Resources  
Research, Chinese Academy of Sciences, 11A, Datun Road,  
Chaoyang District, Beijing 100101, China  
e-mail: hefn@igsnr.ac.cn

S. Li  
e-mail: lisc.10s@igsnr.ac.cn

X. Zhang  
e-mail: xzzhang@igsnr.ac.cn

S. Li  
University of the Chinese Academy of Sciences,  
No. 19A Yuquan Road, Beijing 100049, China

X. Zhang  
Jiangsu Collaborative Innovation Center for Climate Change,  
Nanjing University, 22 Hankou Road, Nanjing 210093,  
Jiangsu, China

## Introduction

It is well known that human activities play an important role in global environmental change (Foley et al. 2005). One of the most important aspects of human activities is the clearing of natural ecosystems for agriculture. At present, more than 30 % of the world's landscapes are under some sort of development, and another 30 % are more or less modified (Vitousek et al. 1997). Such large-scale modifications of the land surface have led to notable earth system changes, including emissions of large amounts of anthropogenic greenhouse gases, losses of biodiversity, land surface energy imbalances and hydrological cycle changes (Ellis et al. 2013). Therefore, at present, there is a large amount of effort being put into quantifying land use and land cover change (LUCC) to assess its earth system impacts, especially in regard to the climate system since the start of the industrial period (He et al. 2014).

Numerical simulations are widely used to study the climatic effects of LUCC (Pitman et al. 2011). Climate models and ecosystem models are spatially explicit. In addition, climate and biogeophysical data are normally presented as maps, which are also spatially explicit representations. Thus, to model the effects of LUCC on climate systems since industrial times, it is imperative to develop spatially explicit datasets of historical LUCC that have been traditionally reconstructed at the level of political units. Therefore, there is a growing body of methods to reconstruct spatially explicit LUCC datasets covering a long time scale.

Using the contemporary and historical inventories of agricultural land and a ‘hindcast modeling’ method, the Center for Sustainability and the Global Environment (SAGE) created a global cropland dataset for 1700–1992 with a resolution of  $0.5^\circ$  (Ramankutty and Foley 1999). The SAGE dataset was updated in 2010 (Ramankutty and Foley 2010). Utilizing historical population density maps as proxies, the History Database of the Global Environment (HYDE) was created by the Netherlands Environmental Assessment Agency (Klein Goldewijk 2001). The latest HYDE 3.1 dataset covers the past 12,000-year period with a grid resolution of  $5'$  and was generated by allocating the political unit-based cropland areas into grids based on a cropland satellite-based map of 2000 and six major factors (Klein Goldewijk et al. 2011). On the basis of the SAGE and HYDE datasets, Pongratz et al. (2008) reconstructed agricultural areas for the last millennium from AD 800 to 1992 using population data as a proxy for agricultural activity. Moreover, Houghton et al. (1999), Houghton (2003) reconstructed the conversion rates for different types of land cover at a global scale based on a book-keeping model. A spatially explicit forest cover dataset of Europe over the last three millennia was created using historical population data and maps of relative land suitability for crops and pastures (Kaplan et al. 2009). There are also other historical reconstructions based on a combination of data and modeling (e.g., Lin et al. 2009; Liu and Tian 2010).

However, as noted by the creator of SAGE dataset, the dataset captures the general patterns of global cropland change over the past 300 years but no local to regional details (Ramankutty and Foley 2010). The uncertainties of the HYDE datasets were also analyzed in terms of five aspects: context and framing, input data on population and land use, model parameters and assumptions, model structure, and model technical details (Klein Goldewijk and Verburg 2013). The regional evaluation for China indicated that the global datasets, e.g., the SAGE and HYDE datasets, poorly captured the regional conditions (He et al. 2013; Li et al. 2010; Zhang et al. 2013).

Liu and Tian (2010) created a dataset including cropland, forestland and urban areas of China at a  $10 \times 10$  km resolution from 1700 to 2005 using satellite-based land cover data and long-term historical document-based estimations. However, as noted by the creator, this dataset is still based on the assumption that the historical spatial patterns of cropland and forestland follow the current patterns. This assumption may be problematic, as suggested by Houghton and Hackler (2003). Recently, there has been progress in several research projects that enables us to revisit these problems. First, more reliable historical cropland area data of China are now available (Feng et al. 2005; Ge et al. 2004; Ye et al. 2009). In addition, with the advances of remote sensing and geographical information system technology, more datasets have been made available to provide more accurate maps of the current crop cover and some natural factors.

Therefore, this paper aims to create a new spatial dataset of cropland with a cell size of  $10 \times 10$  km for China from 1661 to 1996 using a novel method. The paper is organized as follows. Second section introduces the “Materials and methods”. Third section introduces the “Results”. Fourth section introduces the “Uncertainty analysis”, and fifth section introduces the “Discussion and conclusions” respectively.

## Materials and methods

The analysis outline of this paper is summarized in Fig. 1. First, by collecting cropland area data and filling the data gaps, we reconstructed the provincial cropland area dataset of China for 1661–1996. Second, altitude, slope and climate were selected to assess land suitability for cultivation. Next, combined with satellite-based crop cover of the 1980s (Liu et al. 2005), we devised an allocation model of provincial cropland area. Subsequently, based on this model, the provincial cropland area was allocated into  $10 \times 10$  km grids. Finally, comparisons with satellite-based crop cover of 2000 and with the HYDE 3.1 dataset were made to validate our reconstruction.

### Data sources of provincial cropland area

Many studies on the historical cropland area of China have been conducted, but currently, a provincial cropland area dataset covering the entirety of China for 100s of years still does not exist. In this work, on the basis of previous studies and government inventories, we reconstructed a provincial cropland area dataset of the mainland China for 1661–1996 via collection, revision and reconstruction.

**Fig. 1** Flowchart depicting the analysis outline of this study. The boxes with sharp corners indicate data at the level of political units, whereas boxes with rounded corners indicate spatially explicit data

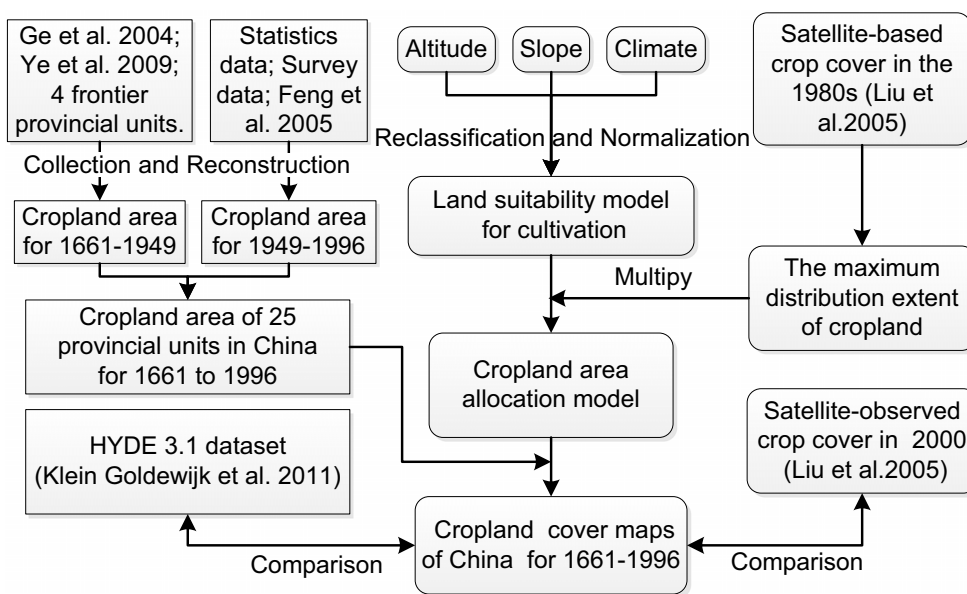
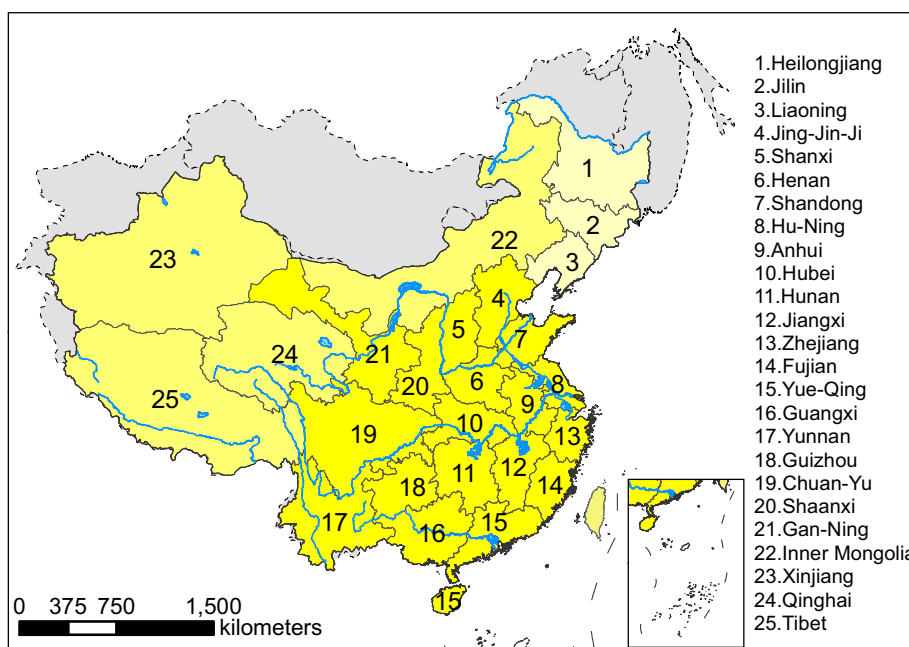


**Fig. 2** Location of the study area. Based on the data sources, the study area consists of three parts: the data of three provincial units numbered 1–3 for 1683–1940 are from Ye et al. (2009); the data of 18 provincial units numbered 4–21 for 1661–1933 are from Ge et al. (2004); the cropland area of four provincial units numbered 22–25 for 1661–1949 was estimated in this study. The gray shaded area is the territory and provincial units of China in the Qing dynasty



*The Qing dynasty and the Republic of China period (1661–1949)*

Our study area is the current People’s Republic of China (Fig. 2). For the three provinces (numbered 1–3 in Fig. 2) in northeast China, the provincial cropland area of 1683–1940 was compiled by Ye et al. (2009; Table 1). For the 18 provincial units (numbered 4–21 in Fig. 2) in the traditionally cultivated region of China, the provincial cropland area of 1661–1933 was compiled by Ge et al. (2004). The data of Ye et al. (2009) and Ge et al. (2004) were rigorously estimated using Chinese historical tax-cropland area records from

historical archives such as Collections of Historical Governmental Archives (《文献通考》) and General Chorography of Shengjing (《盛京通志》). These estimations were based on the harmony of historical data and modern data from the State Statistics Bureau (SSB). Thus, their estimations represent the historical real cropland area and are potentially directly comparable to modern data.

It should be noted that the 18 provincial units described by Ge et al. (2004) are not the same as the current ones. From 1661 to 1933, the territory and provincial units of China changed (Tan 1991; Fig. 2). To combine the data with modern statistics or investigational data, some current

**Table 1** Sources of cropland area data and population data of China from 1661 to 1996

Data	Region	Time slices covered	Spatial resolution	Data source
Cropland	18 provincial units in traditional cultivated region of China	1661, 1685, 1724, 1784, 1820, 1873, 1887, 1893, 1913, 1933	Provincial	Ge et al. (2004)
	Three provincial units of Northeast China	1683, 1735, 1780, 1908, 1914, 1931, 1940	County	Ye et al. (2009)
	Four frontier provincial units of China	1953	Provincial	SSB (1953)
	25 provincial units of China	1949–1960	Provincial	SSB (1950–1961)
	25 provincial units of China	1961–1985	National	Feng et al. (2005)
	25 provincial units of China	1986–1996	Provincial	MLR (1997)
Population	Four frontier province units of China	1776, 1820, 1851, 1880, 1910, 1953	Province	Cao and Ge (2001)

provincial units were merged into history units as follows: ① Beijing, Tianjin and Hebei were merged to form Jing-Jin-Ji; ② Shanghai and Jiangsu were merged to form Hu-Ning; ③ Chongqing and Sichuan were merged to form Chuan-Yu; ④ Hainan and Guangdong were merged to form Yue-Qiong; ⑤ Ningxia and Gansu were merged to form Gan-Ning. These provincial units are consistent with the historical records in the Qing dynasty.

For the four frontier provincial units (numbered 22–25 in Fig. 2) of China, there are no existing cropland area data before 1949. Therefore, estimation was performed in this study. Agriculture is inherently linked to the population (Houghton 1999). In this study, we estimated the provincial cropland area using population data in 1776, 1820, 1851, 1880, 1910, 1953 (Cao and Ge 2001) and the per capita cropland area data of 1953. Cao and Ge (2001) rigorously estimated the historical population based on Chinese historical archive materials such as *Compilation of historical records in the Qing dynasty* (《清实录》) and many Chinese population policies in history. Thus, the data have a high level of confidence. The per capita cropland area of 1953 was calculated in this paper using population and cropland area data in 1953 (Cao and Ge 2001; SBB 1953). The cropland area data in 1953 are the output of the “Land measuring and Yields evaluation” (“查田定产”) policy and can represent agricultural conditions of the initial period of the People’s Republic of China. An assumption that the per capita cropland area remained constant from the Qing dynasty to the initial period of the People’s Republic of China was made, as the four provincial units are sparsely populated and agricultural technology lagged during the past several centuries. Finally, the cropland area of the four provincial units from 1776 to 1910 was calculated according to the per capita cropland area values. For the period of 1661–1776, extrapolation was used based on the cropland area change tendency during 1776–1953. The historical cropland area data of Taiwan are missing.

#### *The People’s Republic of China period (1950–1996)*

For the period after 1949, there are two available data sources of cropland area: the SSB dataset and the Ministry of Land and Resources dataset (1997; hereafter, MLR). The SSB data cover the longest time period without discontinuity, but may largely underestimate the cropland area of China after 1960, which has been widely recognized among experts (Crook 1993; Feng et al. 2005). In this study, the provincial cropland area from SSB was used for 1949–1960.

Since 1987, the MLR annually released Cropland Area Change Data (MLR 1997). These data have a high level of confidence (Feng et al. 2005). In addition, the National Land Use Detailed Survey Data in 1996 (MLR 1997) also have a high level of confidence and have been widely used. Thus, in this study, the Cropland Area Change Data from MLR (1997) and the National Land Use Detailed Survey Data in 1996 (MLR 1997) were used to retrieve the actual cropland area for 1986–1995.

Feng et al. (2005) estimated the national cropland area of China for the period of 1961–1985 based on correlation analysis between food yields and cropland area. The calculation indicated that food yields and cropland area are well correlated during that time period and that SSB food yield data are more accurate than SSB cropland data. Moreover, their estimations were validated against international sources and special periods and cropland-related policies are also well reflected in their results. Thus, using the method developed by Feng et al. (2005), the provincial SSB cropland area for 1961 to 1985 was revised in this study using this correlation analysis.

All of the above collected, reconstructed and revised data were linked together in time and space. Eventually, we obtained the provincial cropland area dataset of mainland China for 1661–1996.

Methods for spatially explicit allocation

As the cropland was characterized by expansion over the past several centuries, the historical cropland was located within the present cropland domain. In this study, the satellite-based cropland data from the 1980s was used to denote the present cropland domain because the cropland area reached a maximum in the 1980s (Feng et al. 2005). In detail, we could determine whether there was cropland in the 10 × 10 km grids through overlaying the grids with 1 km resolution satellite-based cropland data from Liu et al. (2005). As a result, we obtained the present Boolean crop cover extent map  $W_{crop}(i)$ . For  $W_{crop}(i)$ , the value 1 indicates cropland in a given grid and 0 indicates no cropland.

The provincial cropland area was spatially explicitly allocated within the present Boolean crop cover extent map  $W_{crop}(i)$  according to the spatial weight of cropland for each grid with a cell size of 10 × 10 km. The land cultivation history of China indicated that lands with good natural conditions were cultivated first and were followed gradually by marginal lands with harsh natural environments (Han 2012; Wang 2005). That is to say, the spatial weight of cropland for each grid is determined by the land’s natural properties. Therefore, to allocate the provincial cropland area into 10 × 10 km grids, some natural factors were selected to assess the spatial weight of cropland for each grid, which was represented by land suitability for cultivation.

Generally, land suitability for cultivation is jointly determined by topography, climate conditions, soil and the presence of rivers. At the 10 × 10 km grid scale, soil mainly determines whether the land is suitable for cultivation and its effects on cultivation are included in the present cropland domain (Sun and Shi 2003). For China, irrigation has been advanced even in older time periods, especially in the traditionally cultivated regions of China, so the distance from rivers plays only a slight role (Wu 1996). Therefore, in this study, three quantitative factors, i. e., altitude, surface slope, and potential maximum productivity of climate were used to assess land suitability for cultivation.

Altitude will cause the vertical variation of hydrothermal conditions. Generally, along with the increase in altitude, an accumulated temperature  $\geq 10$  °C will decrease at a rate of 150–200 °C/100 m, and the growing season will also be shortened (Department of Economic Geography in Institute of Geography of Chinese Academy of Sciences 1980). In addition, we also found that the satellite-based reclamation rate (i.e., the fraction of cropland area to the total land area in a 1 × 1 km grid) in the 1980s is negatively correlated with altitude, with correlation coefficients higher than -0.5 for 14 provinces. This finding suggests

that land suitability for cultivation decreases with the increase in altitude. Moreover, there are different cultivation patterns at different altitudes because of the vertical differences of hydrothermal conditions. However, within different altitude ranges, the significance of such variations is quite different. Only when the altitude reaches such a height that the crop growth becomes limited by the hydrothermal conditions does it impact cropland distribution (Lin et al. 2009; Sun and Shi 2003). Therefore, we reclassified and reassigned the altitude value according to the standards (Table 2) derived from Sun and Shi (2003). The following Eq. (1) was used to quantify the relationship between altitude and land suitability for cultivation in province  $k_n$  ( $n = 1, 2, 3, \dots, 25$ )

$$D'(i) = \frac{\text{Max}(D(i)) - D(i)}{\text{Max}(D(i))} \tag{1}$$

where  $D'(i)$  is the altitude weight on land suitability for cultivation of grid  $i$ ,  $D(i)$  is the altitude of grid  $i$ , and  $\text{Max}(D(i))$  is the maximum altitude value of grid  $i$ . In addition, the altitude data were cited from the 1 km resolution GTOPO30 dataset.

Surface slope is closely related to soil erosion, land drainage and irrigation. We found that the satellite-based reclamation rate in the 1980s is negatively correlated with surface slope, with correlation coefficients higher than -0.5 for 13 provinces. Generally, no soil erosion occurs when the slope is below 3°. Soil erosion is common when the slope is between 3° and 15°, and serious soil erosion occurs on land with a slope higher than 25° (Sun and Shi 2003). We reclassified and reassigned the slope values as shown in Table 2. The original slope was calculated using the GTOPO30 dataset. The slope weight on land suitability for cultivation of grid cell  $i$  in province  $k_n$  ( $n = 1, 2, 3, \dots, 25$ ),  $S'(i)$ , was calculated as follows:

$$S'(i) = \frac{\text{Max}(S(i)) - S(i)}{\text{Max}(S(i))} \tag{2}$$

**Table 2** Reclassification and reassignment of altitude and slope (Sun and Shi 2003)

Altitude level (m)	Reassigned value (m)	Slope level (°)	Reassigned value (°)
≤100	100	≤2	2
100–250	250	2–6	6
250–500	500	6–15	15
500–750	750	15–25	25
750–1,000	1,000	>25	45
1,000–1,500	1,500		
1,500–2,000	2,000		
2,000–3,000	3,000		
>3,000	4,000		



where  $S'(i)$  is the slope weight on land suitability for cultivation of grid cell  $i$ ,  $S(i)$  is the slope value of grid cell  $i$ , and  $\text{Max}(S(i))$  is the maximum slope value of grid cell  $i$ .

The potential maximum productivity of climate is an index determined by precipitation, temperature and radiation in terms of land suitability for cultivation. This parameter reflects the suitability of climate for cultivation (Smit and Cai 1996). The potential maximum productivity of climate used in this study was the climatology condition (mean of 1951–1980) from the Data Sharing Infrastructure of Earth System Science (<http://www.geodata.cn>). The climate weight on land suitability for cultivation of grid cell  $i$  in province  $k_n$ , was calculated using the following Eq. (3):

$$C'(i) = \frac{C(i)}{\text{Max}(C(i))} \quad (3)$$

where  $C'(i)$  is the climate weight on land suitability for cultivation of grid cell  $i$ ,  $C(i)$  is the climatic potential productivity value of grid cell  $i$ , and  $\text{Max}(C(i))$  is the maximum climatic potential productivity value of grid cell  $i$ .

Using the above-mentioned Boolean crop cover extent map  $W_{\text{crop}}(i)$  and three factors determining land suitability for cultivation, we calculated the spatial weight of cropland for each grid at a size of  $10 \times 10$  km as follows:

$$W(i) = W_{\text{crop}}(i) \cdot D'(i) \cdot S'(i) \cdot C'(i) \quad (4)$$

where  $W(i)$  is the provincial cropland area allocation weight of grid  $i$ .

Then, we normalized the  $W(i)$  in province  $k_n$  using the following Eq. (5) to be sure that the total weight for one province is one.

$$R(i) = W(i) / \sum_i W(i) \quad (5)$$

Finally, we used Eq. (6) to estimate the cropland area within one grid at a size of  $10 \times 10$  km.

$$\text{Crop}(i, t) = R(i) \cdot \text{area}(k_n, t) \quad (6)$$

where  $\text{Crop}(i, t)$  is the cropland area of grid  $i$  in year  $t$ , and  $\text{area}(k_n, t)$  is the cropland area of the province  $k_n$  in year  $t$ .

Few grids at size of  $10 \times 10$  km are fully filled by cropland. Through analysis of the satellite-based crop cover in the 1980s at this scale, we found that the cropland of 97 % of the grid is  $<90 \text{ km}^2$ . Therefore, in the allocation process, we prescribed that the maximum cropland in a grid would not exceed  $90 \text{ km}^2$ . When we detected the cropland area calculated by Eq. (6), we removed all of the excess area and implemented a loop to allocate the area until all of the grids met the prescribed limit of  $90 \text{ km}^2$ .

The above cropland area allocation process was looped for the years 1661, 1685, 1724, 1784, 1820, 1873, 1887, 1893, 1913, 1933, 1940, 1950, 1960, 1970, 1980, 1990 and 1996.

## Results

### Changes of cropland area from 1661 to 1996

#### Changes at the national level

The cropland area increased in mainland China from  $55.5 \times 10^4 \text{ km}^2$  in 1661 to  $130.0 \times 10^4 \text{ km}^2$  in 1996 (Fig. 3). The annual growth rate (hereafter, AGR) is  $0.2 \times 10^4 \text{ km}^2$  (0.25 %). From the national cropland area curve, we could detect a steady growth phase for 1661–1873, and a rapid growth phase with fluctuations for 1873–1996.

From 1661 to 1873, the cropland area increased by  $31.0 \times 10^4 \text{ km}^2$ , with an AGR of 0.21 %. In addition, a growth transition occurred at approximately 1724. From 1661 to 1724, the cropland increased at an AGR of 0.48 %. From 1724 to 1873, it increased only at an AGR of 0.09 %. The high rate of increase for 1661–1724 mainly derived from the reclamation of abandoned cropland from the late Ming dynasty. The low increase rate from 1724 to 1873 was due to the cultivation of virgin land for more food, which is more difficult than reclamation. The cropland area in 1873 was  $86.5 \times 10^4 \text{ km}^2$ .

For 1873–1996, the cropland area increased rapidly with fluctuations at an AGR of 0.33 %. At first, the cropland area continued increasing from 1873 to 1933 followed by a decrease from  $103.7 \times 10^4 \text{ km}^2$  in 1933 to  $100.5 \times 10^4 \text{ km}^2$  in 1950 because of wars and natural disasters. Next, the cropland area increased rapidly at an AGR of 0.99 %, which is the maximum growth rate of the whole study period. In 1980, the cropland area reached its maximum value,  $134.8 \times 10^4 \text{ km}^2$ , of the whole study

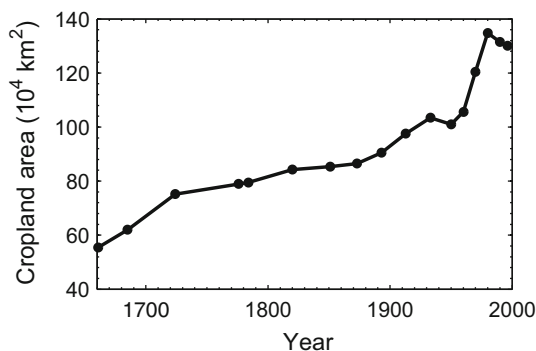


**Fig. 3** Cropland area of mainland China for 1661–1996

period. For 1980–1996, however, the cropland area decreased to  $130.0 \times 10^4 \text{ km}^2$  because of adjustments of agricultural structure and land-use transformations, especially urbanization.

*Changes at the provincial level*

At the provincial level, the increase of cropland area from 1661 to 1996 could be detected in each province, but the magnitudes of the increases were different and the AGRs ranged from 0.01 % in Hu-Ning Province to 2.30 % in Jilin Province (Fig. 4). Northeast China (Heilongjiang, Jilin and Liaoning), southwest China (Chuan-Yu and Guizhou), Inner Mongolia and Xinjiang have AGRs higher than 0.50 %, whereas the provinces located in the middle-lower regions of the Yangtze River basin (Hubei, Jiangxi, Anhui, Hu-Ning and Zhejiang), Shanxi and Shandong Provinces had AGRs lower than 0.10 %.

In addition, an uneven increase rate of each province was also observed in different periods of 1661–1996. For most provinces, the increase had a low (high) rate before (after) the late nineteenth century. In the first period, the cropland area of most provinces in the traditionally cultivated region grew at a slow rate. Only the cropland area of some provinces in the northeast and southwest grew at relatively high rates. In the second period, the cropland increased at an unexpectedly high rate from 1873 to 1980 and dropped obviously after 1980. For 1873–1980, northeastern, southwestern and northwestern China (Xinjiang, Qinghai and Tibet) had large increase rates with a maximum AGR of 2.31 % in Xinjiang. The Gan-Ning and Huang-Huai-Hai Plain (Jing-Jin-Ji, Henan, Shandong and Hu-Ning) had small increase rates with a minimum AGR of -0.11 % in Gan-Ning. For 1980–1996, 20 provinces experienced a decrease in cropland area, most of which are distributed in the mid-east part of China.

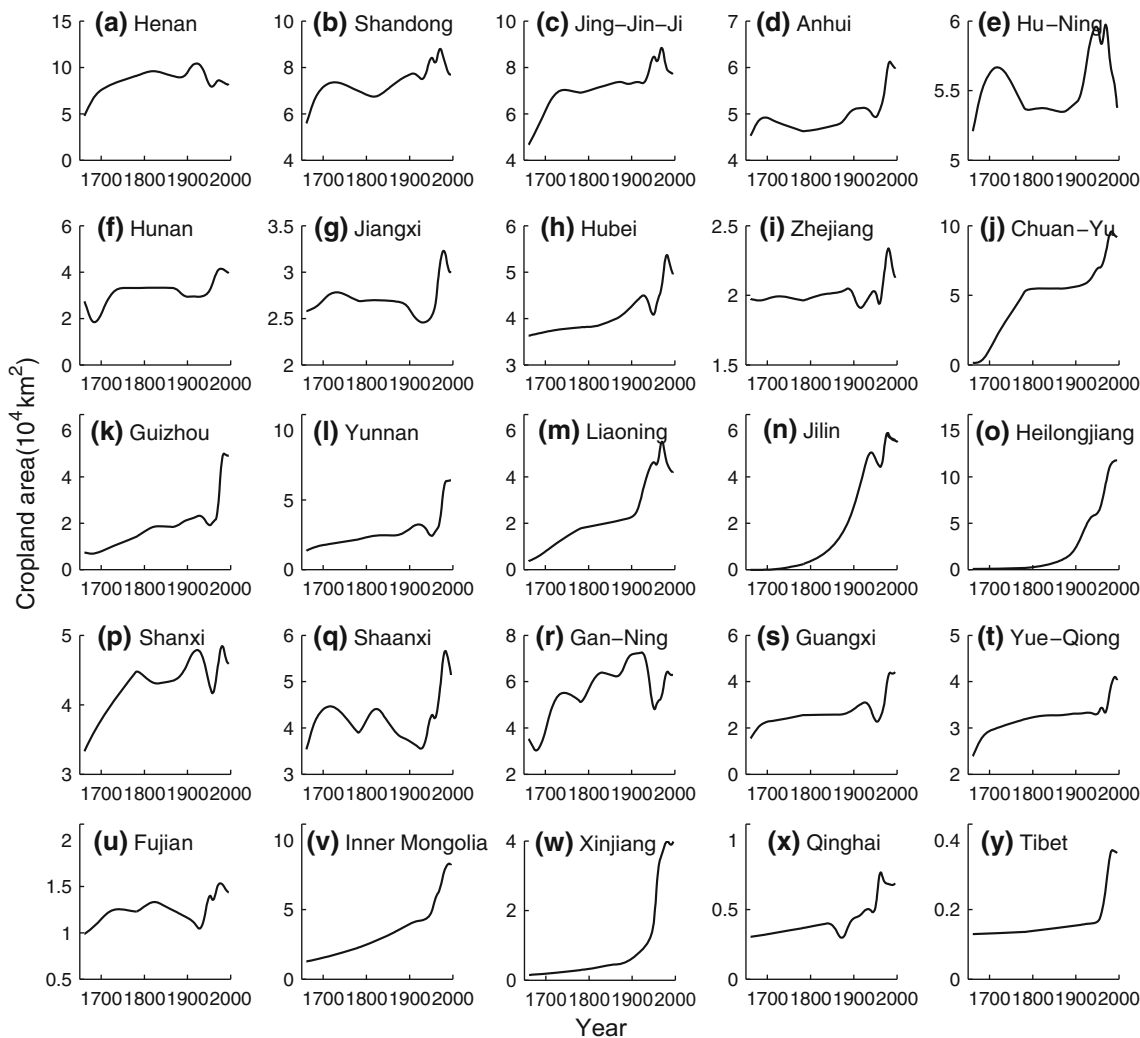


**Fig. 4** Cropland area of each province in mainland China for 1661–1996

### Spatial pattern changes of crop cover from 1661 to 1996

Our grid-based crop cover reconstruction for eight time slices is presented in Fig. 5. In 1661 (Fig. 5a), croplands were mainly limited to the North China Plain, the Guanzhong Basin and the Hanjiang River Valley where ancient Chinese people initially cultivated. The extent of cropland distribution in south China was small, and the agricultural intensification was also at a low level. Subsequently, in 1724 (Fig. 5b), the agriculture intensified in the North China Plain and the Guanzhong Basin, especially the south of Jing-Jin-Ji and south of the Henan Province, which indicates that the abandoned croplands in the late Ming dynasty and the early Qing dynasty, were gradually reclaimed from 1661 to 1724. In addition, the cropland expanded in the Sichuan Basin and the Liaohe Plain.

For 1724–1784 (Fig. 5c), the agriculture in the Sichuan Basin intensified and the agricultural frontier gradually

migrated southward into the Yunnan-Guizhou Plateau. Because of the policy of “Bureaucratization of Native Officers” (“改土归流”) for southwestern China (Chuan-Yu, Guizhou and Yunnan) during Emperor Yongzheng’s reign (1722–1735) in the Qing dynasty, a large number of farmers of the surrounding area were encouraged to cultivate. From 1784 (Fig. 5d) to 1873 (Fig. 5e), the agricultural frontier migrated northeastward into the Jilin and Heilongjiang Provinces and crops can also be found in the oasis region of Xinjiang. From 1873 to 1933 (Fig. 5f), new cultivation was developed extensively in Heilongjiang and the cropland in northeastern China and Xinjiang also largely increased. Such a large increase in cropland resulted from a large level of migration from the Shandong and Henan Provinces. Because of the abolition of the “Prohibit reclamation in Northeast China” (“东北封禁”) policy in 1860 by Emperor Guangxu, farmers from the Shandong and Jing-Jin-Ji areas could migrate freely to northeast China. In addition, the agriculture was also intensified in

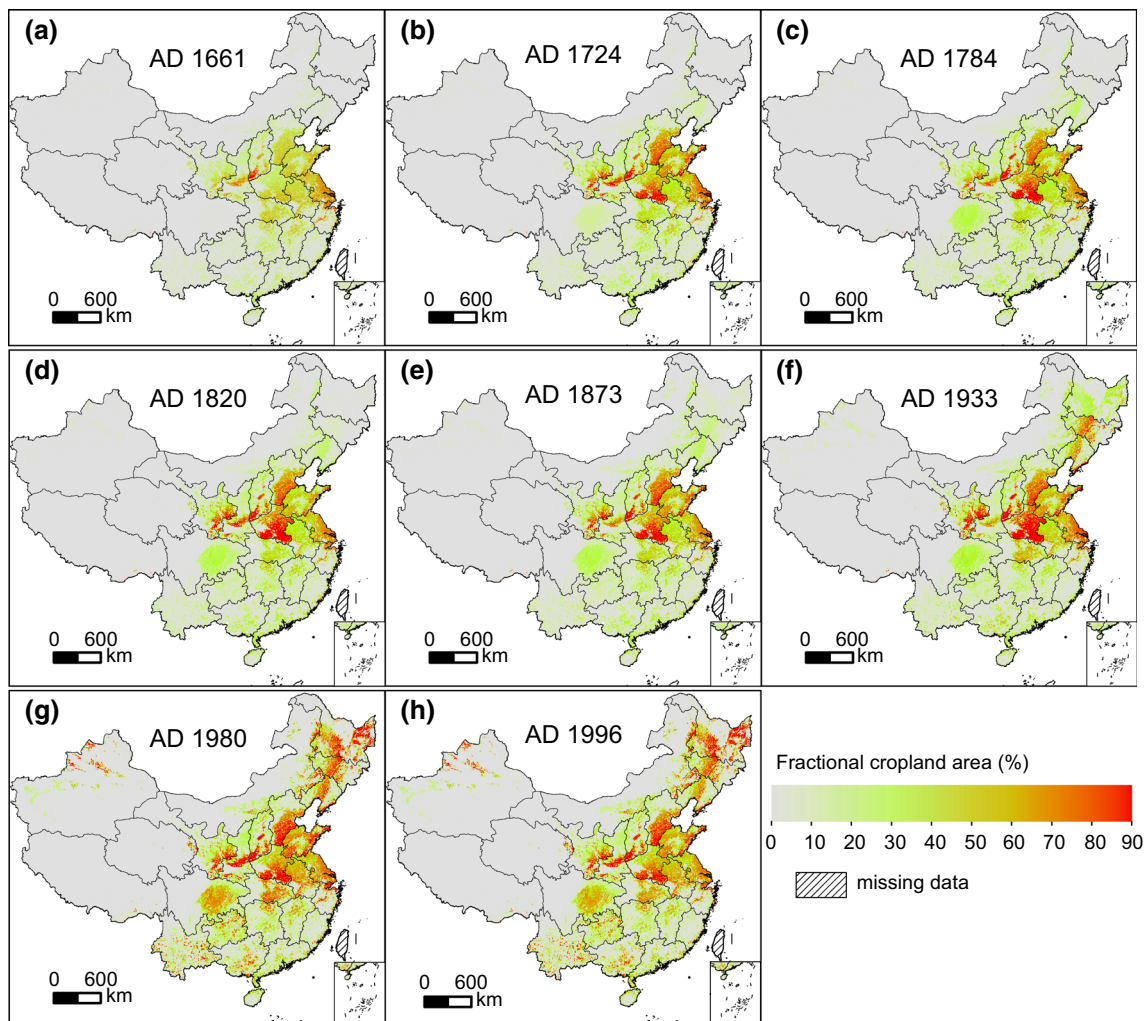


**Fig. 5** Historical crop cover of China mainland for 1661–1996 at  $10 \times 10$  km resolution. The data for Taiwan is missing



the Guangxi and Yunnan Provinces. In 1980 (Fig. 5g), the degree of land reclamation was obviously enhanced in Heilongjiang, the oasis region of Xinjiang and south China. The extent and intensification of the agricultural distribution reached their maximum levels. The main cultivated regions of China are the North China Plain, northeastern China, Sichuan Basin, Yangtze River Basin, Loess Plateau and Pearl River Basin. After 1980, as the economy and urbanization of China developed rapidly, most provinces in the traditionally cultivated region of China experienced a cropland area decrease (Fig. 5h).

### Uncertainty analysis

To assess the uncertainties of our reconstruction quantitatively, we reconstructed the crop cover for the year 2000 by our model, and the provincial cropland area was aggregated from satellite-based crop cover in 2000 (Liu et al. 2005) to ensure they are the same with satellite-based data. Then, we compared our reconstruction for 2000 with satellite-based crop cover for 2000. We also compared our reconstruction with HYDE 3.1 (Klein Goldewijk et al. 2011), a global historical environmental dataset.

#### Comparison with satellite-based data

Comparing our reconstruction (Fig. 6a) with satellite-based data for 2000 (Fig. 6b), we observe that they are close on the whole and that the main agricultural region is northeast China, the North China Plain and the Sichuan Basin. However, some differences between them still exist (Fig. 6c). More cropland is observed in the southeast of Gan-Ning region, the North China Plain, the Sichuan Basin and the Liao-he River Plain for our reconstruction compared to the satellite-based data. Meanwhile, less cropland area is observed in the northwest of Gan-Ning region, the

farming-pastoral zone of China and southern China. In addition, the differences are mostly distributed between  $-20$  and  $+20$  %, and the larger the difference level is, the lower the proportion of the grid numbers (Table 3). The regions with more allocated cropland area in our reconstruction have relatively lower altitudes, whereas the regions with less allocated cropland area have relatively higher altitudes. That finding may indicate that the weighting of topography is slightly high in our reconstruction model.

#### Comparison with HYDE 3.1 dataset

Because of the absence of historical crop cover maps, we are limited to comparisons to other reconstruction studies to validate our dataset, such as the HYDE 3.1 dataset (Klein Goldewijk et al. 2011). The main differences between HYDE 3.1 and our study are that HYDE 3.1 used state level data while we used provincial level data and the reconstruction methods are also different.

Figure 7 illustrates the cropland area of our study and HYDE 3.1 over nearly the past four centuries. Before 1700, the HYDE 3.1 data are higher than our value, but its AGR is lower than our data. For 1700–1930, the magnitudes of the increase of both are similar. After 1930, the magnitudes of the increase in cropland area have some discrepancies. In our study, after a slight decrease from 1930 to 1950, the cropland area increased rapidly for 1950–1980, followed by another slight decrease for 1980–1996. While the HYDE 3.1 steadily increased for 1930–1960 decreased for 1960–1980, and increased rapidly for 1980–2000. Since 1960, based on some previous studies, we revised the statistical data for 1960–1985 and used the inventory data for 1986–1996. However, the data of HYDE 3.1 after 1960 were indirectly cited from the SSB data of China, which may have largely underestimated the cropland area of China (e.g., Crook 1993; Feng et al. 2005).

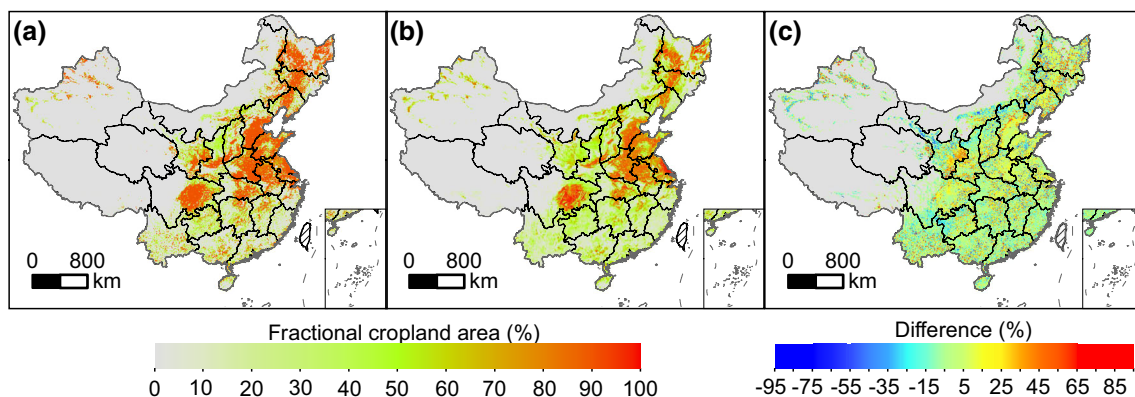


**Fig. 6** Comparisons between our reconstruction and satellite-based data. **a** Reconstructed crop cover for 2000, **b** satellite-based crop cover for 2000, **c** differences between **a**, **b**. The gray shaded area is non-crop area; the data for Taiwan is missing

**Table 3** Statistical classification of differences between our reconstruction and the satellite-based data for 2000

Difference level (%)	[-95, -80)	[-80, -60)	[-60, -40)	[-40, -20)	[-20, 0)	[0, 20)	[20, 40)	[40, 60)	[60, 80)	[80, 95)
Proportion of grid numbers (%)	0.05	0.48	2.42	9.48	42.60	29.00	10.44	4.13	1.23	0.17

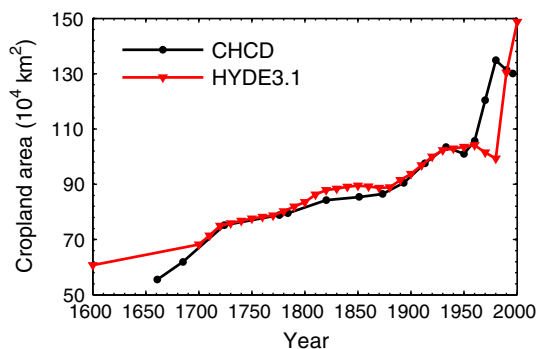
**Fig. 7** Cropland area comparison between our reconstruction Chinese Historical Cropland Dataset (CHCD) and HYDE 3.1 dataset

Figure 8 shows a spatial comparison between our reconstruction and HYDE 3.1 dataset. We observe that in our maps the cropland was mainly distributed in the North China Plain, the Guanzhong Basin and the mid-lower reaches of the Yangtze River Basin for 1724 (Fig. 8a). From 1724 to 1933, the cropland expanded in northeast China and the Sichuan Basin (Fig. 8b, c). From 1933 to 1996, the cropland expanded in the northeast and south of China and into the oasis region of Xinjiang (Fig. 8d). HYDE 3.1 dataset showed the cropland mainly distributed in the mid-lower regions of the Yellow and Yangtze River Basins, the Beijing-Hangzhou Canal coastal areas and the Sichuan Basin for 1720 (Fig. 8e). From 1720 to 1930, the spatial pattern of crop did not change substantially (Fig. 8f, g). And during 1930–2000, sudden changes of crop cover can be detected (Fig. 8g, h), especially the decrease in land-use intensification in many agricultural regions of China, which may be problematic.

Figure 8i–k illustrates that our reconstruction has more cropland area in the south of Gan-Ning, the south of Jing-Jin-Ji and the south of the Henan Province, but less cropland area in the Sichuan Basin, the mid-lower reaches region of Yangtze River Basin and northeastern China. In regard to 2000, the amplitude of the differences in most regions shrink, especially in the Yellow and Yangtze River Basins (Fig. 8l). These differences are most likely because they were developed using different methods. Six major factors were used in the method of HYDE 3.1, including the distance to rivers. Because the negative differences were mostly along the large rivers, HYDE 3.1 may overestimate the weight of distance from rivers in their model (Zhang et al. 2013).

## Discussion and conclusions

### Discussion

This reconstruction was accomplished on the basis of rational assumptions concerning cropland spatial distribution in historical times. However, several uncertainties still exist.

First, there are some uncertainties with the historical provincial cropland area data utilized in this study. For example, the cropland area of Chuan-Yu for 1661 and 1724, which we cited from Ge et al. (2004), may be underestimated because of the issue of non-reporting of cropland in official census data. In the estimation process of the cropland area for the frontier provinces for 1661–1953, we assumed that the per capita cropland area value remained constant from the Qing dynasty to the initial period of People's Republic of China. However, this value perhaps decreased slightly during this period because of the improvements in food production per unit area of land (Han 2012; Ruddiman and Ellis 2009). Collecting more historical information concerning agriculture and the population of these regions will be helpful for future studies.

Moreover, the calculation of the spatial allocation weight and land suitability for cultivation may have some uncertainties. For instance, from Fig. 6c, we can see that positive differences are primarily distributed in plain and basin areas, and negative differences are primarily distributed in mountainous areas. Perhaps the allocation weight of cropland is slightly higher in the plain and basin areas, whereas slightly lower in mountainous areas. In this study, we normalized the altitude, slope and climate factors and integrated them with equal weights to obtain the land suitability value for cultivation, which is a type of initial preprocessing. In the future, more attention should be paid to quantifying the specific relationships between these factors and land suitability for cultivation.

In addition, in the development of land suitability for cultivation assessing model, the traditionally cultivated regions located in the mid-eastern part of China was our major consideration. Several factors possibly affecting land suitability for cultivation in western or northeastern China were not incorporated into our model. For example, in the traditionally cultivated region of China, rainfall is abundant, and the irrigation systems are advanced; therefore, the distance to rivers is not a primary factor affecting land

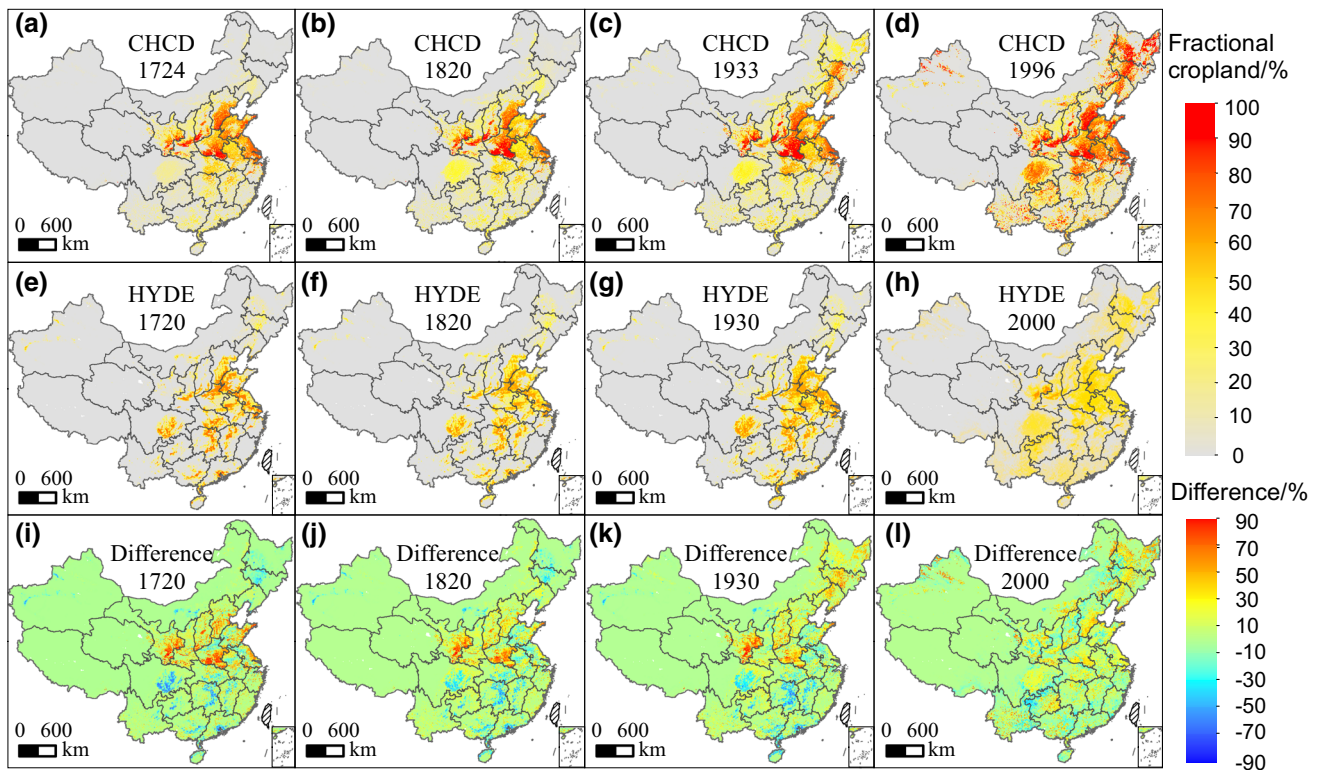


**Fig. 8** Spatial pattern comparison between our reconstruction CHCD and HYDE 3.1 dataset for 1724, 1820, 1933 and 1996

suitability for cultivation. However, in western China, because of the scarce precipitation, the distance to rivers do affect the development of agriculture, which can also be observed from satellite-based crop cover data in the 1980s (Liu et al. 2005). Perhaps, because of the absence of the river factor, uncertainties of cropland distribution may exist in western China.

Developing different models to assess the land suitability for cultivation in different regions of China in future studies and considering more regional scale details will perhaps improve the accuracy of cropland spatial weights.

## Conclusions

The above-mentioned reconstruction indicates that the cropland area of mainland China increased from  $55.5 \times 10^4 \text{ km}^2$  in 1661 to  $130.0 \times 10^4 \text{ km}^2$  in 1996. At the provincial level, the cropland area of all provinces also displays an increasing trend. The  $10 \times 10 \text{ km}$  crop cover datasets of China for 1661–1996 indicate that from 1661 to 1873, the cropland area expanded in the southwest and northeast, especially in the Sichuan Basin. Subsequently, from 1873 to 1980, the agricultural frontier expanded northeastward and southward, and land reclamation greatly intensified. During the whole process, agriculture gradually intensified in the North China Plain. After 1980, most

provinces in the traditionally cultivated region of China experienced slight decreases in cropland area.

Our reconstruction and the satellite-based data in 2000 are close on the whole. And differences are mostly distributed between  $-20$  and  $+20\%$ . Compared with HYDE 3.1, our model is more suitable for reconstructing the historical crop cover of China at  $10 \times 10 \text{ km}$  grid scale.

Our reconstruction could serve as underlying land use/cover data in studying the impact of historical LUCC on climate and in calculating carbon emissions from historical LUCC over the past several centuries.

**Acknowledgments** This research was supported by the National Natural Science Foundation of China (Grant No. 41271227), the China Global Change Research Program (Grant No. 2010CB950901) of the Ministry of Science and Technology of China and the National Natural Science Foundation of China (Grant No. 41471171).

## References

- Cao S, Ge J (2001) China population history, vol V. Qing dynasties. Fudan University Press, Shanghai
- Crook F (1993) Underreporting of China's cultivated land area: implications for world agricultural trade. In: China International Agricultural and Trade Report, situation outlook ser RS-93-4. United States Department of Agriculture, Washington, DC, pp 33–39

- Department of Economic Geography in Institute of Geography of Chinese Academy of Sciences (1980) Chinese general agricultural geography. Science Press, Beijing
- Ellis E, Kaplan J, Fuller D, Vavrus S, Klein Goldewijk K, Verburg PH (2013) Used planet: a global history. *Proc Natl Acad Sci USA* 110:7978–7985. doi:[10.1073/pnas.1217241110](https://doi.org/10.1073/pnas.1217241110)
- Feng Z, Liu B, Yang Y (2005) A study of the changing trend of chinese cultivated land amount and data reconstructing: 1949–2003. *J Nat Resou* 20:35–43
- Foley JA et al (2005) Global consequences of land use. *Science* 309:570–574. doi:[10.1126/science.1111772](https://doi.org/10.1126/science.1111772)
- Ge Q, Dai J, He F, Zheng J, Man Z, Zhao Y (2004) Spatiotemporal dynamics of reclamation and cultivation and its driving factors in parts of China during the last three centuries. *Prog Nat Sci* 14:605–613. doi:[10.1080/10020070412331344021](https://doi.org/10.1080/10020070412331344021)
- Han M (2012) Historical agricultural geography of China. Peking University Press, Beijing
- He F, Li S, Zhang X, Ge Q, Dai J (2013) Comparisons of cropland area from multiple datasets over the past 300 years in the traditional cultivated region of China. *J Geogr Sci* 23:978–990. doi:[10.1007/s11442-013-1057-z](https://doi.org/10.1007/s11442-013-1057-z)
- He F, Vavrus S, Kutzbach J, Ruddiman W, Kaplan J, Krumhardt K (2014) Simulating global and local surface temperature changes due to Holocene anthropogenic land cover change. *Geophys Res Lett* 41:623–631. doi:[10.1002/2013gl058085](https://doi.org/10.1002/2013gl058085)
- Houghton RA (1999) The annual net flux of carbon to the atmosphere from changes in land use 1850–1990. *Tellus Ser B Chem Phys Meteorol* 51:298–313. doi:[10.1034/j.1600-0889.1999.00013.x](https://doi.org/10.1034/j.1600-0889.1999.00013.x)
- Houghton RA (2003) Revised estimates of the annual net flux of carbon to the atmosphere from changes in land use and land management 1850–2000. *Tellus Ser B Chem Phys Meteorol* 55:378–390. doi:[10.1034/j.1600-0889.2003.01450.x](https://doi.org/10.1034/j.1600-0889.2003.01450.x)
- Houghton RA, Hackler JL (2003) Sources and sinks of carbon from land-use change in China. *Glob Biogeochem Cycle* 17. doi:[10.1029/2002gb001970](https://doi.org/10.1029/2002gb001970)
- Houghton RA, Hackler JL, Lawrence KT (1999) The US carbon budget: contributions from land-use change. *Science* 285:574–578. doi:[10.1126/science.285.5427.574](https://doi.org/10.1126/science.285.5427.574)
- Kaplan JO, Krumhardt KM, Zimmermann N (2009) The prehistoric and preindustrial deforestation of Europe. *Quat Sci Rev* 28:3016–3034. doi:[10.1016/j.quascirev.2009.09.028](https://doi.org/10.1016/j.quascirev.2009.09.028)
- Klein Goldewijk K (2001) Estimating global land use change over the past 300 years: the HYDE database. *Glob Biogeochem Cycle* 15:417–433. doi:[10.1029/1999gb001232](https://doi.org/10.1029/1999gb001232)
- Klein Goldewijk K, Verburg PH (2013) Uncertainties in global-scale reconstructions of historical land use: an illustration using the HYDE data set. *Landsc Ecol* 28:861–877. doi:[10.1007/s10980-013-9877-x](https://doi.org/10.1007/s10980-013-9877-x)
- Klein Goldewijk K, Beusen A, van Drecht G, de Vos M (2011) The HYDE 3.1 spatially explicit database of human-induced global land-use change over the past 12,000 years. *Glob Ecol Biogeogr* 20:73–86. doi:[10.1111/j.1466-8238.2010.00587.x](https://doi.org/10.1111/j.1466-8238.2010.00587.x)
- Li B, Fang X, Ye Y, Zhang X (2010) Accuracy assessment of global historical cropland datasets based on regional reconstructed historical data—a case study in Northeast China. *Sci China Ser D Earth Sci* 53:1689–1699. doi:[10.1007/s11430-010-4053-5](https://doi.org/10.1007/s11430-010-4053-5)
- Lin S, Zheng J, He F (2009) Gridding cropland data reconstruction over the agricultural region of China in 1820. *J Geogr Sci* 19:36–48. doi:[10.1007/s11442-009-0036-x](https://doi.org/10.1007/s11442-009-0036-x)
- Liu M, Tian H (2010) China's land cover and land use change from 1700 to 2005: estimations from high-resolution satellite data and historical archives. *Glob Biogeochem Cycle* 24:GB3003. doi:[10.1029/2009gb003687](https://doi.org/10.1029/2009gb003687)
- Liu J et al (2005) Spatial and temporal patterns of China's cropland during 1990–2000: an analysis based on Landsat™ data. *Remote Sens Environ* 98:442–456. doi:[10.1016/j.rse.2005.08.012](https://doi.org/10.1016/j.rse.2005.08.012)
- Ministry of Land and Resources of China (MLR) (1997) Annual report on Chinese land resources. Geological Publishing House, Beijing
- Pitman AJ, Avila F, Abramowitz G, Wang Y, Phipps S, de Noblet-Ducoudre N (2011) Importance of background climate in determining impact of land-cover change on regional climate. *Nat Clim Chang* 1:472–475. doi:[10.1038/nclimate1294](https://doi.org/10.1038/nclimate1294)
- Pongratz J, Reick C, Raddatz T, Claussen M (2008) A reconstruction of global agricultural areas and land cover for the last millennium. *Glob Biogeochem Cycle* 22. doi:[10.1029/2007gb003153](https://doi.org/10.1029/2007gb003153)
- Ramankutty N, Foley JA (1999) Estimating historical changes in global land cover: croplands from 1700 to 1992. *Glob Biogeochem Cycle* 13:997–1027. doi:[10.1029/1999gb900046](https://doi.org/10.1029/1999gb900046)
- Ramankutty N, Foley J (2010) ISLSCP II historical croplands cover, 1700–1992. In Hall, Forest G, Collatz G, Meeson B, Los S, Brown de Colstoun E, Landis D (eds) ISLSCP initiative II collection data set. Oak Ridge National Laboratory Distributed Active Archive Center, Oak Ridge, p 10. doi:[10.3334/ORNLDAAC/966](https://doi.org/10.3334/ORNLDAAC/966). <http://daac.ornl.gov/>
- Ruddiman WF, Ellis EC (2009) Effect of per-capita land use changes on Holocene forest clearance and CO<sub>2</sub> emissions. *Quat Sci Rev* 28:3011–3015. doi:[10.1016/j.quascirev.2009.05.022](https://doi.org/10.1016/j.quascirev.2009.05.022)
- Smit B, Cai Y (1996) Climate change and agriculture in China. *Glob Environ Chang* 6:205–214
- State Statistical Bureau (SSB) (1950–1997) Statistical yearbook of China. China Statistical Publisher House, Beijing
- Sun H, Shi Y (2003) China agricultural land use. Jiangsu Science and Technology Press, Nanjing
- Tan Q (1991) Concise historical atlas of China. SinoMaps Press, Beijing
- Vitousek PM, Mooney HA, Lubchenco J, Melillo JM (1997) Human domination of Earth's ecosystems. *Science* 277:494–499. doi:[10.1126/science.277.5325.494](https://doi.org/10.1126/science.277.5325.494)
- Wang Y (2005) Chinese historical land use. In: Wang G, Wang J, Wang P (eds) Proceedings of Wang Yuhu. China Agricultural Press, Beijing, pp 310–342
- Wu C (1996) Chinese agricultural history. Police-Education Press, Beijing
- Ye Y, Fang X, Ren Y, Zhang X, Chen L (2009) Cropland cover change in Northeast China during the past 300 years. *Sci China Ser D Earth Sci* 52:1172–1182. doi:[10.1007/s11430-009-0118-8](https://doi.org/10.1007/s11430-009-0118-8)
- Zhang X, He F, Li S (2013) Reconstructed cropland in the mid-eleventh century in the traditional agricultural area of China: implications of comparisons among datasets. *Reg Environ Chang* 13:969–977. doi:[10.1007/s10113-012-0390-6](https://doi.org/10.1007/s10113-012-0390-6)